MONTANA STATE UNIVERSITY LIBRARY

A Comparison of Methods Reveals that Enhanced Diffusion Helps Explain Cold-Season Soil CO 2 Efflux in a Lodgepole Pine Ecosystem

Authors: F. Aaron Rains, Paul C. Stoy, Christopher M. Welch, Cliff Montagne, and Brian McGlynn

NOTICE: this is the author's version of a work that was accepted for publication in Cold Regions Science and Technology. Changes resulting from the publishing process, such as peer review, editing, corrections, structural formatting, and other quality control mechanisms may not be reflected in this document. Changes may have been made to this work since it was submitted for publication. A definitive version was subsequently published in Cold Regions Science and Technology, Volume 121, January 2016, DOI#10.1016/j.coldregions.2015.10.003.

Rains, F. Aaron, Paul C. Stoy, Christopher M. Welch, Cliff Montagne, and Brian L. McGlynn. "A Comparison of Methods Reveals that Enhanced Diffusion Helps Explain Cold-Season Soil CO 2 Efflux in a Lodgepole Pine Ecosystem." Cold Regions Science and Technology 121 (January 2016): 16-24.

Made available through Montana State University's ScholarWorks
scholarworks.montana.edu

A Comparison of Methods Reveals that Enhanced Diffusion Helps Explain Cold-Season Soil CO_2 Efflux in a Lodgepole Pine Ecosystem

F. Aaron Rains [a], Paul C. Stoy [a,*], Christopher M. Welch [a], Cliff Montagne [a], Brian L. McGlynn [b]

[a] Department of Land Resources and Environmental Sciences, Montana State University, Bozeman, MT 59717, USA
[b] Nicholas School of the Environment, Duke University, Durham, NC 27708, USA

A B S T R A C T

Wintertime respiration contributes significantly to the annual loss of carbon from terrestrial ecosystems to the atmosphere, but the magnitude and physical transport mechanisms of this flux through snow remain unclear. Here, we quantify wintertime soil CO_2 efflux in a Lodgepole pine (*Pinus contorta* Dougl.) forest by comparing chamber, flux gradient, and subcanopy eddy covariance measurements. CO_2 efflux estimates from the flux gradient system deviated from the eddy covariance measurements during early and late winter but were only *ca.* 25% lower than eddy covariance measurements during the main snow accumulation period in mid-winter. During the snow-covered period, the flux gradient carbon efflux estimate (15 g C m^{-2}) was *ca.* three-fold less than eddy covariance measurements (49 g C m^{-2}). An analysis of the relationship between friction velocity and eddy covariance-measured CO_2 efflux lends support to the notion that advection through snow is an important transport mechanism for trace gasses. A spectral Granger causality analysis indicates that the wind speed time series contributes information to the subnivean CO_2 concentration time series during the melt period at time scales greater than 10 hours. All three methodologies indicate that wintertime respiration is a major contributor to the annual carbon budget: the sum of eddy covariance-measured CO_2 efflux during the snow-covered period was 1/3 of that during the snow-free period of 2011 (*ca.* 140 g C m^{-2}). Future studies should incorporate adjustments for advection when using snow flux gradient systems to avoid underestimating the often-underappreciated contribution of the cold season to ecosystem CO_2 efflux.

1. Introduction

Soil respiration is the largest contributor to terrestrial CO_2 efflux and returns approximately 80 Pg C to the atmosphere annually (Raich et al., 2002; Schlesinger and Andrews, 2000). Soil CO_2 flux is the dominant respiratory flux in forested ecosystems (e.g. Schäfer et al., 2003), but most studies focus on observations during seasons when belowground metabolic processes are more active. The wintertime portion of the carbon cycle was often considered to be negligible due to a reduction in the primary drivers of soil respiration – soil temperature, labile carbon, and soil liquid water – which hinder metabolic processes within the autotrophic and heterotrophic communities found in the soil medium (e.g. Coyne and Kelley, 1971). Recent studies have demonstrated, however, that cold season respiration is non-trivial (Sommerfeld et al., 1993), and often contributes *ca.* 10–40% or more of the annual CO_2 efflux in ecosystems with seasonal snow cover (Larsen et al., 2007; McDowell et al., 2000; Merbold et al., 2012). With much of the terrestrial surface (on average 46 million km^2) being covered in snow during some portion of the year, cold season CO_2 flux is increasingly recognized as an important component of the terrestrial carbon cycle (Wang et al., 2011).

Snow insulates soil and soil respiration tends to increase with snow depth as a result (Grogan and Jonasson, 2006; Larsen et al., 2007; Monson et al., 2006b), suggesting a close interplay between the physical properties of snow and the biological process of soil respiration. While soil CO_2 efflux responds to changes in snow depth and density throughout the snow-covered season (Monson et al., 2006b), important uncertainties remain in our understanding of how trace gasses move through temporally dynamic snowpacks. As a consequence, the best method to measure CO_2 flux through snow, especially in remote and cold environments, remains unclear.

Several techniques are available for measuring wintertime CO_2 efflux, each with benefits and disadvantages. Chamber measurements can provide highly accurate flux observations but may disturb snow structure, especially if snow is removed for a direct soil CO_2 efflux measurement. Chambers also measure over small scales in space and time and are difficult to automate for continuous measurements during the snow-covered season. Flux gradient methods based on Fick's first law of diffusion can readily provide continuous estimates of wintertime soil CO_2 efflux, but models of the conductance of snow to trace gas diffusion rely on uncertain parameterizations, especially regarding

tortuosity. Recent studies have also demonstrated the non-trivial role of advection through snow, especially due to pressure pumping under windier conditions (Bowling and Massman, 2011), but flux gradient systems in soil or snow rarely account for non-diffusive transport (e.g. Daly et al., 2009).

The observed relationship between wind and CO_2 efflux from the snowpack to the atmosphere also complicates the application of the eddy covariance technique, which must filter out data collected under conditions of insufficient turbulent flux, often approximated as periods with insufficient friction velocity (u_*, Barford et al., 2001), itself related to wind speed. In other words, a variable that is related to wind speed is often used to decide if eddy covariance measurements should be filtered out of the time series, which complicates the ability to ascertain relationships between flux and the changes in wind speed that may cause pressure pumping. Few studies to date have combined the eddy covariance method with flux gradient and chamber measurements during the snow-covered season (but see Monson et al., 2006a), despite the growing prominence of the eddy covariance methodology for quantifying surface–atmosphere CO_2 exchange (Baldocchi, 2008).

In light of these methodological challenges, multi-method comparisons for wintertime CO_2 efflux have been carried out, highlighting the advantages and disadvantages associated with different measurement approaches as well as the important roles of snow cover, climate, and ecosystem type in determining flux magnitude. For instance, McDowell et al. (2000) showed that the chamber on snow method, which required the least amount of disturbance and made the fewest assumptions in comparison to chambers on soil and flux gradient techniques, was the most reliable despite the challenge of making continuous measurements across time. Björkman et al. (2010) compared wintertime efflux sampling methodologies using chamber on both snow and soil surfaces and flux gradient measurements at multiple depths at two sites in Svalbard that differed in elevation and latitude. CO_2 flux estimates from different methodologies differed by up to two orders of magnitude, suggesting that further investigations into measurement methodology are necessary to constrain wintertime CO_2 flux. Furthermore, the divergent efflux estimates are cause for concern because these data are often used in climate models and carbon budget calculations.

Understanding the advantages of various efflux measurement techniques is critical for accurately measuring fluxes, and measuring continuously over time can gain insight into ecosystem functioning. For instance, Monson et al. (2006a) found that wintertime respiration accounted for 7–10% of total annual ecosystem respiration in a subalpine forest. Of particular significance was the snowmelt period when melt water began infiltrating the soil profile; a slight increase in soil temperature of 0.3–0.5 °C resulted in a six-fold increase in respiration. These results demonstrate that the snowmelt period is of particular importance to cold season CO_2 efflux, but also may be prone to advective flux if preferential air flow channels through the snow arise (Merbold et al., 2013).

In the present study, CO_2 efflux observations were made in a Lodgepole pine (*Pinus contorta* Dougl.) stand during the winters of 2010–11 and 2011–12. Snow-surface chamber, flux gradient, and eddy covariance measurement techniques are compared, with a focus on relationships among different techniques during different periods of snowpack development and ablation during the 2011–12 season. We analyze the applicability and representative uncertainties of each sensor system in cold environments given the multiple constraints faced when making measurements as frequently as possible during winter at a remote location. Additionally, we examined the relationship between u_* and eddy covariance-measured CO_2 efflux during both winter and summer periods using the algorithm of Reichstein et al. (2005) to ascertain 1) if unique relationships between u_* and CO_2 efflux existed during the winter season that are consistent with pressure pumping and advective flux through snow (Bowling and Massman, 2011) and 2) the possibility that flux gradient methods may underestimate wintertime CO_2 efflux as a result. We further quantify if subcanopy wind and subnivean pressure (P_{snow}) 'causes' patterns of subnivean CO_2 concentrations (hereafter [CO_2]) using both Granger causality and spectral Granger causality to gain insight into the processes that control the variability in [CO_2].

2. Methods

2.1. Study Site

This study was conducted in the Stringer Creek catchment, a subwatershed within the Tenderfoot Creek Experimental Forest (TCEF) in the Little Belt Mountains of west-central Montana, USA. TCEF encompasses 3591 ha and elevation ranges from 1840 to 2421 m with a mean of 2205 m. Recent research at TCEF has explored soil and ecosystem CO_2 flux at point to watershed scales (Pacific et al., 2009; Pacific et al., 2011; Riveros-Iregui and McGlynn, 2009; Riveros-Iregui et al., 2007; Riveros-Iregui et al., 2008; Riveros-Iregui et al., 2011). Sites were located on a forested plot within the Upper Stringer Creek sub-catchment, a 555 ha catchment with varying range of slope, aspect, and topographic convergence/divergence with extensive experimental infrastructure (Farnes, 1995; Jencso et al., 2009; Pacific et al., 2008).

Average annual precipitation at TCEF is 883 mm, of which 52% falls between October and March and is largely stored as snow until spring melt. Snow depths at the research site during peak accumulation average *ca.* 1–1.5 m and daily mean temperatures during periods when snow is likely to range from 1.7 °C in October, to −12.8 °C in January (Farnes, 1995). Lodgepole pine is the dominant tree species found at TCEF, with minor contributions of subalpine fir (*Abies lasiocarpa* (Hooker) Nuttall), Engelmann spruce (*Picea engelmanni* Parry ex Engelm.), whitebark pine (*Pinus albicaulis* Englem.), and quaking aspen (*Populus tremuloides* Michx.) (Farnes, 1995).

2.2. Micrometeorological Instrumentation

A 3 m micrometeorological/eddy covariance tower was installed below the forest canopy in the fall of 2010 at N46.95218 W110.88507. Soil temperature was measured using a Type T (Copper-Constantan) thermocouple 5 cm below the soil surface. Soil moisture was measured using a CS616 soil moisture probe (Campbell Scientific, Logan, UT, USA; hereafter CSI), likewise installed at 5 cm below the soil surface. Incident and outgoing shortwave and longwave radiation were measured using an NR01 four-component net radiometer (Hukseflux, Delft, The Netherlands), and soil heat flux was measured using an HFP01 heat flux plate (Hukseflux) placed 5 cm below the soil surface. Air temperature and relative humidity were measured using an HMP45C temperature/relative humidity sensor (Vaisala, Vantaa, Finland) and subnivean air pressure at the soil surface (i.e. underneath the snowpack, P_{snow}) was measured using a PTB110 barometer (Vaisala). Snow depth was recorded using a SR50A-L sonic depth sensor (CSI). One-minute averages of all micrometeorological measurements were recorded using CR3000 and CR1000 data loggers (CSI), and half-hourly averages were calculated for comparison with the eddy covariance observations.

2.3. Eddy Covariance

The eddy covariance method measures momentum, H_2O flux, and trace gas flux, here of CO_2. The subcanopy eddy covariance tower was designed to measure CO_2 fluxes representative of soil autotrophic and heterotrophic respiration (Misson et al., 2007), including CO_2 efflux to the atmosphere during winter. The tower was equipped with an enclosed LI-7200 CO_2/H_2O infrared gas analyzer (LiCor, Lincoln, NE, USA) and a CSAT-3 Sonic Anemometer (CSI) both at 2 m above the ground surface. The tube between the air inlet and the LI-7200 was

1 m in length, the flow rate was 14.0 L/min, and the separation between the center of the southward-facing anemometer and the tube inlet was 25 cm northward 5 cm eastward, and 6 cm in the vertical. Measurements were collected at 10 Hz and stored on a CR3000 data logger (CSI). Thirty-minute flux sums were calculated using EddyPro v 4.0 (LiCor). Axes were rotated for tilt correction using double rotation (Lee et al., 2005), time lags were detected using covariance maximization (Mauder and Foken, 2004), and analytic corrections for low pass and high pass filtering effects were applied (Moncrieff et al., 1997; Moncrieff et al., 2005). Statistical tests for raw (10 Hz) data screening (Vickers and Mahrt, 1997) were performed under the 'Statistical Analysis' option in EddyPro. Spike count/removal options were set allowing for a maximum of 3 consecutive outliers. The percentage of accepted spikes per interval was 1.0%, and remaining spikes were replaced by linear interpolation. Eddy covariance measurements of CO_2 flux are subsequently abbreviated F_{EC}.

The eddy covariance methodology assumes that sufficient turbulent kinetic energy is produced such that vertical and horizontal advection is negligible and the surface–atmosphere exchange of CO_2 is dominated by vertical turbulent transport. In practice, this is not always the case, and periods for which insufficient turbulence exists must be identified and removed from the data record. A common method is to identify periods of insufficient turbulence is to use u* as a surrogate for the production of turbulent kinetic energy, and find the minimum value of u* – the u* threshold – at which flux is no longer related to u* (Barford et al., 2001; Papale et al., 2006). The thresholding algorithm of Reichstein et al. (2005) (hereafter the 'Reichstein algorithm') was applied to the data to explore the dependency of F_{EC} on u_*. Briefly, the Reichstein algorithm tests the dependency of F_{EC} on u_* using 3-month subsets of the data. F_{EC} measurements were sorted into temperature and u_* classes. The u_* threshold for each 3-month period was determined to be the u_* value at which mean F_{EC} exceeds 95% of mean F_{EC} at higher u_* values after taking into account the role of temperature in determining the magnitude of F_{EC} (Stoy et al., 2006). The purpose of the u* threshold analysis is to explore if unique relationships between F_{EC} on u* exist during winter that may be consistent with advection caused by pressure pumping through snow (Bowling and Massman, 2011). Namely, a u* threshold value that is higher in winter than during non-snow-covered periods suggests that an increase in subcanopy wind velocity results in an increase in CO_2 efflux and thereby advective transport through snow from pressure pumping.

2.4. Subnivean CO_2 Sampling Instrumentation

A subnivean CO_2 sampling apparatus was installed in the autumn of 2011. A diaphragm pump cycled air at 1 L/min through 0.635 cm vinyl tubing from the ground surface to a fixed GMP 343 CO_2 probe (Vaisala) situated in an airtight case (Pelican Products Inc., Torrance, CA, USA) above the snow surface. The gas was then returned to the subnivean airspace near the inlet port. This design allowed us to prevent the small amount of heat typically produced by solid-state CO_2 sensors from disturbing snow properties *in situ* and from inducing advection by continuously removing gas from the bottom of the snowpack. Measurements were made every minute and averaged to half-hourly periods. Observations were used in conjunction with snow diffusivity estimates, and atmospheric [CO_2] and snow depth measurements from the micrometeorological/eddy covariance tower located *ca*. 5 m away to create a flux gradient system for measuring CO_2 efflux through snow.

2.5. The Flux Gradient Method

The flux gradient approach used here follows Sommerfeld et al. (1993) (see also Seok et al., 2009; Liptzin et al., 2009) and applies Fick's first law of diffusion to estimate surface–atmosphere CO_2 efflux. Assuming neither a net sink nor source of CO_2 in snow itself, Fick's law for the case of CO_2 flux through snow can be written:

$$F_{FG} = -D_{CO2}\frac{dC}{dz} \quad (1)$$

where F_{FG} is the flux gradient estimate of CO_2 flux (μmol m^{-2} s^{-1}), D_{CO2} is the diffusivity of CO_2 through a given medium, here the snowpack, and dC is the difference in CO_2 concentration between two points, here subnivean and atmospheric [CO_2], separated by a difference in-depth dz, here snow depth.

D_{CO2}, was calculated using

$$D_{CO2} = \Phi\tau D(P_0/P)(T/T_0)^{\alpha}, \quad (2)$$

where $D = 0.1381 \times 10^{-4}$ m^{-2} s^{-1} is the diffusion coefficient for CO_2 at standard temperature and pressure ($T_0 = 273$ K and $P_0 = 101.3$ kPa), P is the ambient barometric pressure (here taken to be the pressure of the air space within the snowpack, i.e. P_{snow}), T is the temperature of the snowpack (K), and $\alpha = 1.81$ is a theoretical coefficient (Massman, 1998). Snowpack porosity (Φ) was calculated using $\Phi = 1 - (\rho_{snow}/\rho_{ice})$ (Eisenberg and Kauzmann, 2005), where ρ_{snow} is the mean density of the snowpack and ρ_{ice} is 917 kg m^{-3}. The tortuosity constant τ is based on the empirical relationship $\tau = \Phi^{1/3}$ developed by Millington (1959), although other studies have investigated tortuosity equations that range from $\Phi^{1/3}$ to $\Phi^{2/3}$. Per this definition of tortuosity, τ is greater than zero and less than or equal to one as discussed by Massman and Sommerfeld (1997).

2.6. Snow Chamber Measurements

A PP Systems EGM-4 infrared gas analyzer (IRGA) was used in conjunction with a snow surface chamber and float for chamber-based measurements of CO_2 efflux ($F_{Chamber}$) using the closed chamber method. The float was designed to position the chamber on the snow surface and was constructed of 3.81 cm PVC tubing and wire mesh that housed a 10 L PVC dome-shaped chamber (Sterilite, Townsend, MA) that extended 2.5 cm into the snow to provide a temporary seal against rapid gas transport into or out of the chamber. Two ports in the chamber created a semi-closed loop with 0.635 cm vinyl tubing to be connected to the inlet and outlet ports on the IRGA. A small fan was used to circulate gas evenly throughout the chamber. CO_2 concentration observations were made every 10 seconds for a 5-minute period, and fluxes were calculated using the linear relationship between CO_2 concentration and time. $F_{Chamber}$ measurements were taken in triplicate at monthly intervals within 20 m of the tower during the 2011–12 winter season, although due to complications with power systems only two periods are available for analysis.

2.7. Snow Property Measurements

Snow profile pits were dug in triplicate during each visit to the field site, *ca*. once per month over the course of the winter. Pits were dug no closer than 5 m and no further than 50 m away from the instrumentation arrays and chamber measurement sites. Temperature and snow density were measured at 10 cm increments using a Prosnow kit (Snowmetrics, Fort Collins, CO). Pit location was chosen at random upon each visit to the site, and pits were refilled after measurements were taken to minimize site disturbance. Manual snow density measurements were compared against snow depth and water equivalent measurements from the Onion Park SNOTEL site, located in TCEF near N46.9167 W110.85 (Serreze et al., 1999). A <2% difference in ρ_{snow} was found between monthly pit measurements and corresponding SNOTEL observations. ρ_{snow} derived from SNOTEL was subsequently used for the calculation of Φ. Results are discussed in reference to the

water year, defined as the period from October 1 of the previous year to September 30 of the calendar year. Data that extend beyond a single water year are presented as the fraction of a given (calendar) year.

2.8. Granger Causality in the Time and Spectral Domains

The original definition of Granger causality was given by Granger (1969), "if some other series y_t contains information in past terms that helps in the prediction of x_t, and if this information is contained in no other series used in the predictor, then y_t is said to cause x_t." In practice, establishing Granger causality amounts to a series of Student's *t*-tests and *F*-tests on lagged time series to identify if a univariate model of a given time series x_t is improved using a multivariate model that incorporates y_t. Spectral Granger causality extends such inference to the frequency domain (Geweke, 1982) to ask if information in a given spectral signal Granger-causes a different signal. Significant spectral Granger causality is typically determined using Monte Carlo methods, and we apply iterative amplitude adjusted Fourier transform (IAAFT) surrogates (Schreiber and Schmitz, 1996; Schreiber and Schmitz, 2000) following Venema et al. (2006) as suggested by Detto et al. (2012). IAAFT surrogates preserve the probability distribution, power spectra, and linear correlation structure of the time series (e.g. Molini et al., 2010) such that random spectral signals with identical statistical features to the signals of interest can be created for establishing significance, here at $P < 0.05$. We explore whether snow and atmospheric conditions consistent with pressure pumping were related to $[CO_2]$ by testing if u^* and P_{snow} Granger-cause $[CO_2]$ in the time and spectral domains, and also if $[CO_2]$ Granger-causes u^* and P_{snow}, which would suggest that simple unidirectional causality is a poor descriptor of the dynamics of the system.

3. Results

3.1. Snow Depth, Density, and Water Equivalent

Snow water equivalent (SWE) at the Onion Park SNOTEL site was consistently greater than the 19-year average during water year 2011 and was near the 19-year average during water year 2012 (Fig. 1). Snow depth reached a maximum of 1.2 m in mid-March at the study site during 2012 (Fig. 2). The snowpack melted completely by mid-May and was followed by a late spring snowstorm that melted within a week. Snowpack density increased over time as snow accumulated and settled, with an average range of 0.25 g/cm^3 in late December to nearly 0.4 g/cm^3 in early April (Fig. 2).

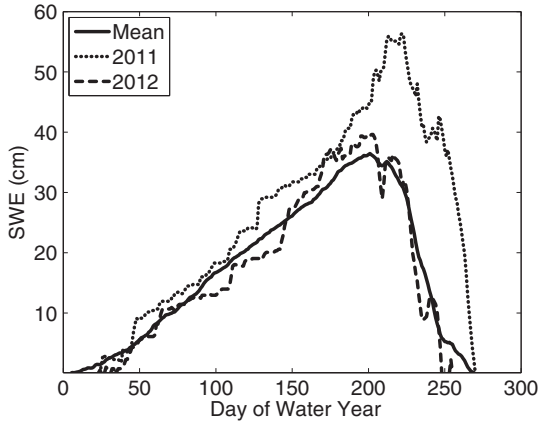


Fig. 1. Snow water equivalent (SWE) measurements from the Onion Park SNOTEL site, MT. Mean SWE refers to the 19-year average and years refers to water years.

3.2. Meteorological and micrometeorological observations

Average to below-average precipitation and average to warm temperatures prevailed during the winter of 2011–12 across Montana and most of the Rocky Mountains of the US and Canada. During the period ranging from December 2011 through May 2012, 166 mm of precipitation fell at TCEF and the average air temperature was 2.2 °C. These values varied from the 20th century mean by −2.8 mm and +2.9 °C, respectively. For the measurement period beginning in late November 2011 and ending in mid-May 2012, air temperatures were typically below 0 °C until early March when daytime temperatures began to climb above freezing (Fig. 3A). Mean soil temperatures at 5 cm belowground were *ca.* −1 °C until mid-March when they climbed above freezing (Fig. 3B). Soil moisture increased in concert with soil temperature as frozen soil water began to melt and snow water began to percolate into the soil (Fig. 3C).

3.3. Eddy Covariance

F_{EC} averaged 0.15–0.18 μmol m^{-2} s^{-1} during the snow accumulation period between late November, 2011 and mid-March, 2012 (Table 1, Fig. 4), and the variance of measured flux increased over time during this period. F_{EC} averaged 0.42 μmol m^{-2} s^{-1} during the snow melt period, over double the average observation during the snow accumulation period, and averaged 0.83 μmol m^{-2} s^{-1} during the month after melt (Table 1).

The u_* threshold calculated by the Reichstein algorithm for summer periods was 0.05 m s^{-1}, near the median value (0.06 m s^{-1}) determined for multiple subcanopy eddy covariance sites by Misson et al. (2007) (Fig. 5). The u_* threshold was determined to be *ca* 0.15 m s^{-1} during the winter of 2010–11 and *ca.* 0.2 m s^{-1} during the winter of 2011–12; i.e. the relationship between u_* and F_{EC} did not saturate until values that exceed the summertime u_* threshold were reached (Figs. 5 and 6). Flux observations were subsequently filtered using the summertime u_* threshold, 0.05 m s^{-1}, assuming that the increase in F_{EC} with u_* is due to enhanced diffusion rather than an underestimation of fluxes due to u_* values below the 0.05 m s^{-1} threshold. No dependency of u_* on F_{FG} was found, excluding values of $u_* < 0.01$ m s^{-1} that were observed infrequently (Fig. 6).

3.4. Subnivean CO_2 Concentration Observations

The subnivean $[CO_2]$ observations exhibited five unique periods (Fig. 7 and Table 1) that were related to snow dynamics. Early-season subnivean $[CO_2]$ (Period I) were usually near the atmospheric $[CO_2]$ of *ca*. 390 ppm with frequent positive excursions, and snow depth was consistently *ca.* 0.4 m. Period II was characterized by steadily increasing subnivean $[CO_2]$ with frequent negative excursions to atmospheric values and a snow depth of approximately 0.65 m with infrequent snowfall events. Period III occurred during the peak snow depth period and exhibited slowly increasing subnivean $[CO_2]$ with relatively low variance compared to other periods (Table 1). Subnivean $[CO_2]$ never dropped to atmospheric values during Period III. Period IV corresponds to the main snowmelt period and was characterized by the mean daily air temperature warming to above freezing, an influx of snow water into the soil, an increasing availability of melting soil water (Fig. 3), an isothermal snowpack, and extensive variability in subnivean $[CO_2]$ concentrations with frequent negative excursions to atmospheric $[CO_2]$. Period V occurred after snow melted and features a small pulse in $[CO_2]$ during the late spring snow event (Fig. 7).

3.5. Flux Gradient

F_{FG} was analyzed based on the five distinct periods observed in the subnivean $[CO_2]$ (Figs. 4 and 7, Table 1). The mean subnivean $[CO_2]$ during Period I was 427 ppm, and concentrations returned to near

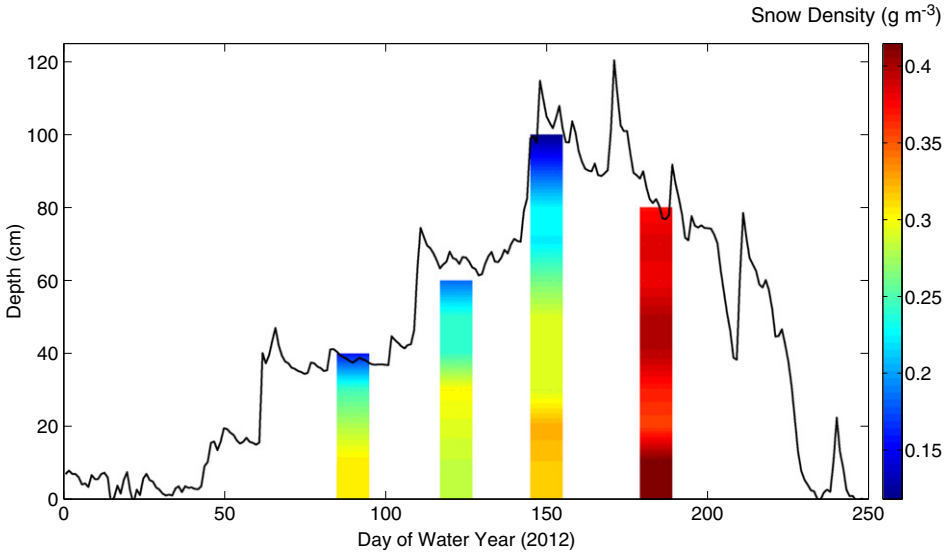


Fig. 2. Snow depth observations from a tower-mounted sonic distance sensor and snow density (g cm^{-3}) at 10 cm increments at the Tenderfoot Creek Experimental Forest research site during the 2012 water year.

atmospheric concentrations (<400 ppm) during *ca* 30% of the Period I measurement record. The mean F_{FG} during Period I was 0.04 μmol CO_2 m^{-2} s^{-1}. As snow depth increased to >0.4 m during Periods II and III, subnivean [CO_2] largely remained at levels above atmospheric [CO_2]. Mean F_{FG} for these periods increased three-fold to *ca*. 0.13 μmol CO_2 m^{-2} s^{-1}. Subnivean [CO_2] was on average slightly lower during Period IV and F_{FG} averaged 0.10 μmol CO_2 m^{-2} s^{-1}, with higher variance (Table 1). The flux gradient approach was not applicable during most of Period V due to lack of snow (Figs. 1, 2, and 7).

3.6. Chamber Measurements

Successful $F_{Chamber}$ measurements were made during two of the field site visits on January 31, 2012 and April 3, 2012. The mid-winter $F_{Chamber}$ in late January had a mean of 0.65 μmol CO_2 m^{-2} s^{-1} and a standard deviation of 0.043 μmol CO_2 m^{-2} s^{-1}. The springtime $F_{Chamber}$ measurements made in early April had a mean of 1.31 μmol CO_2 m^{-2} s^{-1}, approximately double that of the January measurements, and a standard deviation of 0.22 μmol CO_2 m^{-2} s^{-1} (Fig. 4).

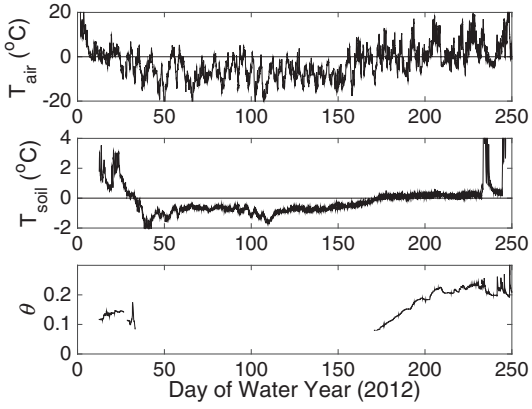


Fig. 3. (A) Air temperature at 2 m above the soil surface (T_{air}), (B) soil temperature at 5 cm below the soil surface (T_{soil}), and (C) volumetric soil moisture content (θ) for the snow-covered period of the 2012 water year in a Lodgepole pine forest at the Tenderfoot Creek Experimental Forest, MT. θ observations for frozen soil conditions have been excluded.

3.7. Intercomparison Among Methods

Each of the three techniques applied in this study resulted in different estimates of seasonal flux dynamics. Mean F_{FG} was on average 75% of F_{EC} during Periods II and III, but only *ca*. 25% of F_{EC} during Periods I and IV (Fig. 4, Table 1). Results indicate that the flux gradient approach approximates eddy covariance-measured fluxes well during winter periods experiencing an aggrading snow pack with a depth over *ca*. 0.4 m, and without the occurrence of significant melt periods. The low values of F_{FG} during Periods I and IV are due in part to the large excursions of subnivean [CO_2] to values near atmospheric (Fig. 7), which diminishes dC (Eq. (1)). $F_{Chamber}$ measurements taken during both Period III and Period IV were not statistically different from concomitant F_{EC} measurements (two-sided *t*-test, $P > 0.05$), but were significantly greater than concomitant F_{FG} observations ($P < 0.05$).

3.8. Granger Causality in the Time and Spectral Domains

Wind speed measurements did not Granger-cause subnivean [CO_2] in the time domain during Period IV when F_{FC} was large and subnivean [CO_2] was temporally dynamic. P_{snow} Granger-caused subnivean [CO_2], and subnivean [CO_2] Granger-caused P_{snow}. Results suggest complicated Granger causality in the time domain due to the complex periodicity of the signals, and as a consequence spectral Granger causality was tested to explore if the spectral signatures of wind speed and subnivean pressure were useful for explaining patterns of subnivean [CO_2] in the frequency domain. Results demonstrate that wind speed, but not subnivean pressure, Granger-caused [CO_2] at frequencies lower than 0.1 $hours^{-1}$ (i.e. time scales greater than 10 hours) at the 95% confidence level (Fig. 8).

4. Discussion

Soil respiration in winter is often thought to be muted but may contribute substantially to ecosystem carbon outputs (Monson et al., 2006a; Oechel et al., 1998). We compared chamber, flux gradient and eddy covariance methodologies in an effort to determine the accuracy, effectiveness, and applicability of each technique for the purpose of better-understanding controls on wintertime soil CO_2 efflux. Results demonstrate that each approach has benefits and disadvantages, with implications for interpreting the contributions of wintertime CO_2 efflux

Table 1
The mean (μ) and standard deviation (σ) of CO_2 flux measurements using flux gradient (F_{FG}) and eddy covariance (F_{EC}) systems for different periods of the 2012 water year. Periods were identified by the statistics of subnivean [CO_2] dynamics (Fig. 7). Units for μ and σ are μmol CO_2 m^{-2} s^{-1} and units for flux sums (Σ) are g C per square meter.

		F_{FG}			F_{EC}		
Period	Dates (m/d/y)	μ	σ	Σ	μ	σ	Σ
I	11/23/2011–01/18/2012	0.041	0.0024	1.0	0.15	0.041	3.7
II	01/18/2012–02/16/2012	0.13	0.0030	3.8	0.17	0.037	5.0
III	02/16/2012–03/16/2012	0.13	0.0013	4.0	0.18	0.070	5.5
IV	03/16/2012–05/14/2012	0.10	0.0097	6.0	0.42	0.25	25.2
V	05/14/2012–06/30/2012	–	–	–	0.83	0.62	
I–IV	11/23/2011–05/14/2012	0.082	0.082	14.9	0.27	0.44	49.0
Snow free	7/2/2011–11/7/2011	–	–	–	1.03	1.03	137

to the carbon balance of forested ecosystems. We discuss and compare findings from each methodology, followed by a discussion of the spectral analysis of the patterns of subnivean [CO_2] during the melt period to identify potential contributions of wind and subnivean pressure variations to the venting of the snow air space.

4.1. Eddy Covariance

The u_* threshold of 0.05 m s^{-1} identified during summertime periods by the Reichstein algorithm (Fig. 5) agrees with u_* threshold values found for other subcanopy eddy covariance systems, which averaged 0.06 m s^{-1} (Misson et al., 2007). However, the u_* thresholds for the winter periods of 2011 and 2012, *ca.* 0.15–0.2 m s^{-1}, indicate that flux during winter has a higher dependency on u*, itself related to wind speed (Figs. 5–6). These observations support the hypothesis that wind-enhanced transport is likely a contributing factor in wintertime CO_2 flux (Bowling and Massman, 2011) because increased friction velocity enhanced flux during snow-covered periods, but not during summer over the observed 0.05 m s^{-1} u_* threshold.

4.2. Subnivean CO_2 Observations and the Flux Gradient Method

At low heights above the ground, the eddy covariance approach may slightly underestimate total flux if contributions to surface–atmosphere exchange from eddies characterized by short time and length scales cannot be resolved. F_{EC} thus likely represents an underestimate of the true CO_2 efflux as the contributions of eddies with characteristic time

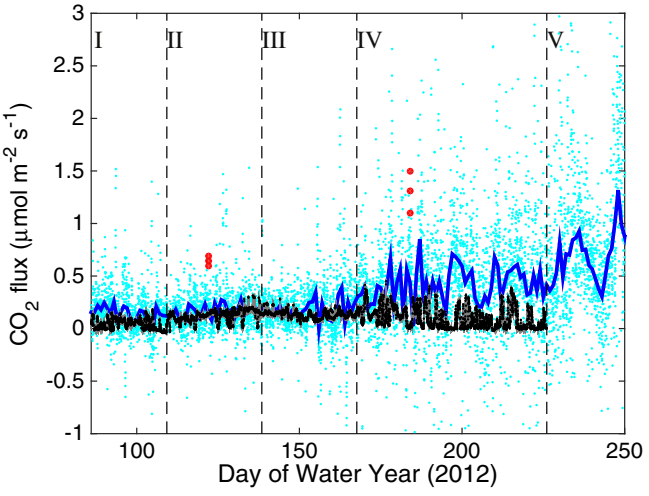


Fig. 4. CO_2 flux estimates calculated using Fick's first law of diffusion from observations from a flux gradient system (black line), half-hourly (cyan dots), and daily averaged (blue line) eddy covariance CO_2 flux measurements, and chamber flux measurements (red dots). A sensitivity analysis of the tortuosity parameter for the flux gradient system is presented as a gray region about the black line.

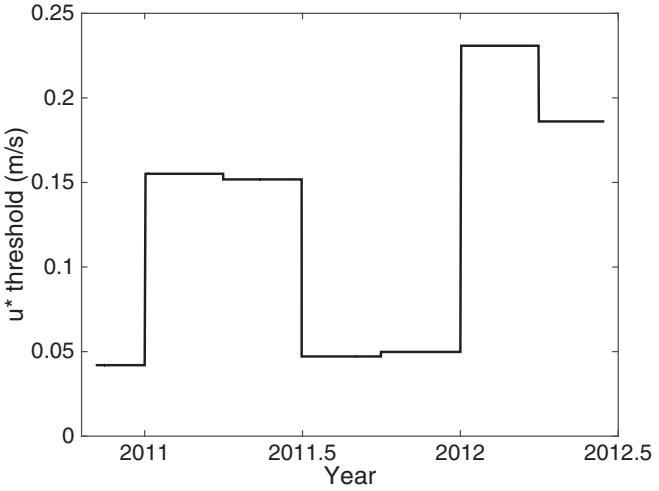


Fig. 5. Temporal changes in the eddy covariance friction velocity (u_*) threshold (m/s) determined using the algorithm of Reichstein et al. (2005).

scales at frequencies larger than 10 Hz cannot be measured with our experimental design; increasing the frequency resolution of the eddy covariance system to 20 Hz would have resulted in missing data during the melt period, when the site was difficult to access, due to limitations in data storage in the CR3000. However, the flux gradient method exhibited a further 25% negative bias compared to eddy covariance measurements during the main snow accumulation period (Periods II and III, Table 1) and larger biases during the remaining periods. These observations warrant an investigation of the uncertainties in the flux gradient methodology.

Uncertainties in snow depth, *dz* in Eq. (1), scales inversely with flux gradient CO_2 flux estimates. Snow depth was measured continuously using a SR50A sonic distance sensor (CSI) with a vertical accuracy of $\pm$ 1 cm. This measurement of snow depth, effectively at a point, contrasts the variable height of the snowpack within the variable eddy covariance flux footprint. The assumption that sonic distance sensor observations are representative of snow depth in the area of the flux tower can be tested using snow pit observations as a surrogate for spatial variability of snow depth across the study site. The mean observed snow pit depth did not differ by more than 5.4 cm from the sonic distance sensor measurements during any single measurement period,

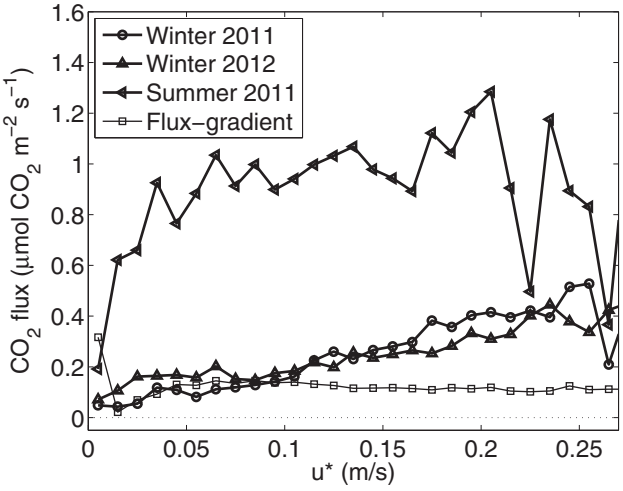


Fig. 6. Eddy covariance and flux gradient CO_2 flux measurements as a function of the friction velocity (u_*). Eddy covariance data are shown for periods during the snow-free season in 2011 (between July 1 and October 19, 2011) and during the snow-covered periods of water years 2011 and 2012.

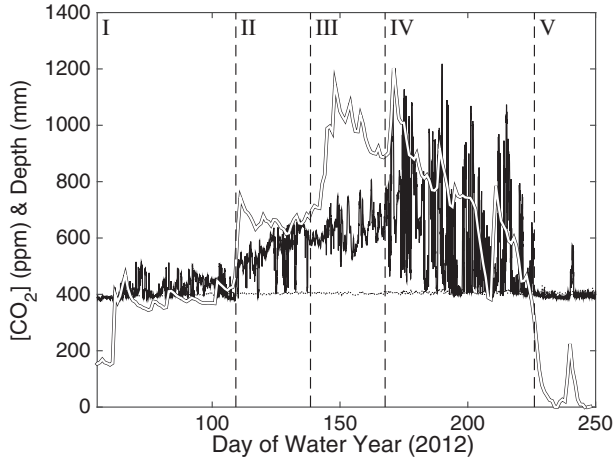


Fig. 7. The relationship between subnivean $[CO_2]$ (solid), atmospheric $[CO_2]$ (dotted), and snow depth (black borders) at the TCEF Lodgepole pine forest site during the 2012 water year. Measurements were made on a half-hourly basis. Subnivean CO_2 concentration measurements fall into five statistically distinct periods described further in Table 1.

with a mean difference of 1.6 cm across all observations. For a snow depth of 1 m, the uncertainties in flux gradient CO_2 flux estimates that these uncertainties in-depth incur are on the order of 1–6%. Errors in the snow depth measurement are not likely to be a dominant source of error in F_{FG} at our site.

Another source of uncertainty in the flux gradient calculation is the subnivean/atmospheric gradient in $[CO_2]$, dC. Uncertainties in the measurements of atmospheric $[CO_2]$ by the LiCor 7200 infrared gas analyzer are on the order of 1% and are unlikely to be a dominant contributor to uncertainty in the flux gradient calculation. The GMP343 used for subnivean $[CO_2]$ measurements has uncertainties on the order of 3% within the temperature range of −40 to 60 °C, and on the order of 10 ppm within the pressure range of 700 hPa to 1300 hPa. Combined, uncertainty in dC measurements is unlikely to be greater than 5%, noting also any biases in dC scale linearly with F_{FG}. Uncertainties in the measurements of dC/dz are alone insufficient to explain the proposed negative bias in F_{FG} estimates during Periods II and III that is likely to be at least 25%.

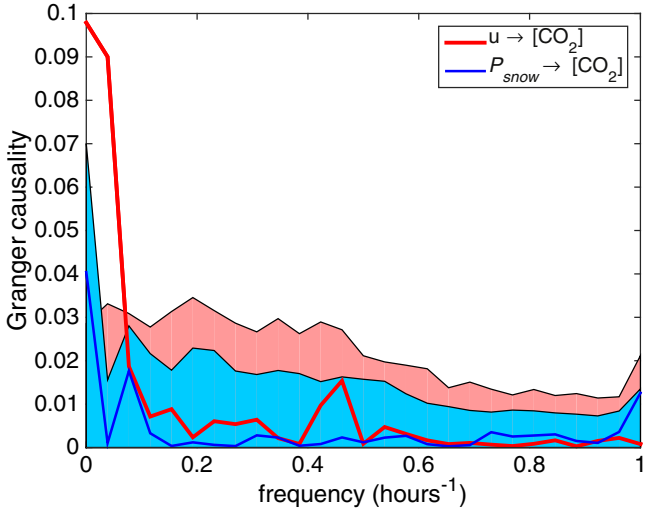


Fig. 8. Granger causality in the spectral domain for the effects of subcanopy wind speed (u) on subnivean $[CO_2]$ and subnivean air pressure (P_{snow}) on $[CO_2]$. Confidence intervals at the 95% percentile for u Granger-causing $[CO_2]$ (pink) and P_{snow} Granger-causing $[CO_2]$ (light blue) were calculated using 1000 iterative amplitude adjusted Fourier transform (IAAFT) surrogates for each variable.

On the other hand, the model for D_{CO2} (Eq. (2)) contains numerous sources of bias that may contribute to the proposed underestimation of F_{FG}. Temperature and pressure adjustments to the atmospheric diffusivity of CO_2 (i.e. D in Eq. (2)) are unlikely to contribute substantial uncertainty to D_{CO2}, and thereby flux gradient estimates, if these inputs are measured within a few percent of the true value. The temperature and air pressure of the snowpack was measured continuously and minor uncertainties due to these observations will not account for a 25% flux underestimation. The Eisenberg and Kauzmann (1969) model for Φ is theoretically consistent because it describes the percent of air space in a snowpack under the assumption that snow density measurements account for the liquid and solid phases of water in the snow, the remainder is the air space within the snow, and that a snowpack without gaseous or liquid components is ice. It is reasonable to assume that these assumptions hold at the snowpack scale, and therefore that uncertainties in the snow density measurement, rather than the equation itself, are the dominant source of uncertainty in Φ. Field measurements of snow density with proper practice are likely accurate to within 5–10% if care is taken with the snow pit or snow tube measurements. It is important to note that these uncertainties, whereas small, also factor into the calculation of τ.

Models for τ show satisfactory agreement with field observations and theoretical expectations (Millington, 1959; Millington and Quirk, 1961) and have been found to be appropriate descriptors of trace gas fluxes in soil and snow (Striegl and Ishii, 1989), but may contain uncertainties that may bias the F_{FG} estimate. Tortuosity values ranging from 0.74 to 0.94 (Using $\tau = \Phi^{1/3}$) were observed during the entire study period, with a mean of 0.92 during the main snow accumulation Periods II and III. In other words, the entire range of observed τ differs by *ca.* 30%, and F_{FG} and F_{EC} differed by an average of *ca.* 25% during Periods II and III. However, a 25% upward adjustment to the median tortuosity value of 0.9 equals *ca.* 1.1, which exceeds the range possible values of τ following the definition used here (Massman and Sommerfeld, 1997). A sensitivity analysis of τ between a range of observed values between 0.74 and 0.94 (Mast and Wickland, 1998; Sommerfeld et al., 1993) was unable to explain the discrepancy between F_{FG} and F_{EC} (Fig. 4), suggesting that variation in tortuosity alone cannot account for the potential underestimation of F_{FG}. Combining inference from measurement systems and setting Eq. (1) to equal F_{EC} rather than F_{FG} resulted in a mean estimate of τ that was greater than one, further suggesting that τ alone is insufficient to account for the potential underestimate of F_{FG}. It is important to note that eddy covariance uncertainty is on the order of 10–15% (Goulden et al., 1997), which again does not explain the full discrepancy between measurement systems.

A final explanation for the underestimation observed in Periods II and III is that the flux gradient method does not account for an enhanced diffusion (i.e. advection), caused by wind-induced pressure pumping of the air space (Bowling and Massman, 2011). From our observations, mean F_{FG} and F_{EC} were approximately equal for u_* values between *ca.* 0.03 and 0.11 m/s during winter 2012 (Fig. 6). F_{FG} was characteristically less than F_{EC} at values above 0.15 m/s, suggesting that wind-enhanced gas transport likely played a role in the underestimation of F_{FG}. In fact, Bowling and Massman (2011) were able to explain the dynamics of stable isotopic composition within the snowpack at their Niwot Ridge study site by adjusting flux gradient estimates of CO_2 efflux for variations in above canopy wind speed. Their upward adjustment based on wind speed resulted in a 20–30% increase in flux. Likewise, Seok et al. (2009) found that under windy conditions, flux gradient-estimated fluxes dropped to as low as 13% of the magnitude of fluxes measured under non-windy conditions.

A plausible explanation for the discrepancy in observations, especially during the melt period (Period IV), may be the creation of preferential flow pathways through the snowpack via macropores created by snow-surface melt-water percolation and snow thawing/refreezing (Merbold et al., 2013). Median subnivean $[CO_2]$ was typically between 650 and 700 ppm during daytime hours (between 900 and 1730)

when warmer temperatures may melt preferential flow paths but was between 700 and 810 ppm during all other periods. Later during the melt period, when the snowpack was shallower, the exposure of understory vegetation and other preferential allows gas to escape rapidly to the atmosphere unobstructed rather than via diffusion through the snowpack matrix. These conditions violate the assumptions of the flux gradient methodology that gas is transported from soil surface to atmosphere via diffusion (Eq. (1)). Taking these observations into account, we have determined that the flux gradient method is most appropriately applied in mid-winter situations at our study site, and that correction for enhanced diffusion will further result in more defensible flux estimates during these periods.

4.3. Snow Chamber Measurements

The snow chamber technique is potentially the most accurate means of sampling flux from the snow surface (McDowell et al., 2000) because one physically samples the increase in CO_2 concentration over time in a known volume and makes no assumptions regarding the resistance of the snowpack to gas transport nor the characteristic time scales of flux-transporting eddies in the atmosphere. A primary drawback of chamber techniques is that one must be physically present at the field site to perform manual sampling or design a complicated automated chamber system that must account for changes in snow depth across the snow-covered season. Such an automated system will likely have large power requirements, which may additionally limit applicability in areas where grid access is unavailable and alternate power sources may be difficult to access. Other potential drawbacks include altering subnivean pressure dynamics by disturbing snow structure when approaching a measurement site. Where site access is a non-issue, chamber techniques provide a relatively low cost and very accurate means of snow surface flux sampling.

4.4. Granger Causality

The spectral Granger causality analysis indicates that patterns in wind speed Granger-caused patterns in $[CO_2]$ at time scales greater than 10 hours (frequencies lower than 0.1 $hour^{-1}$) during Period IV. This result is similar to the findings of Massman and Frank (2006), who found time lags between tens to hundreds of hours between forcing (wind speed) and response (subnivean $[CO_2]$). We found little evidence for a 'trigger' of $[CO_2]$ by large excursions in wind speed and thereby surface pressure over short time scales. An implication of our findings is that any correction for enhanced diffusion for the purpose of improving flux gradient systems should consider the frequency dynamics of atmospheric forcings in addition to any observed relationships between wind speed and $[CO_2]$ in the time domain. Future studies should further investigate 3D advection and diffusion of trace gasses through the complex snow medium (Huwald et al., 2012; Massman, 2006) as induced by pressure pumping (Clarke and Waddington, 1991) and explore parameterizations for enhanced diffusion based on both above- and subcanopy wind speed observations to make existing corrections (Bowling and Massman, 2011) more widely applicable for different canopy types.

5. Conclusion

Wintertime CO_2 efflux has proven to be an important contributor to the annual carbon cycle at in many ecosystems dominated by seasonal snow cover. Determining the most efficient and cost-effective means of measuring these processes will allow researchers to conduct more in-depth and widespread inquiries into the evolution of wintertime CO_2 flux processes. This study compared eddy covariance, flux gradient, and chamber methodologies for measuring wintertime CO_2 efflux in a forested ecosystem. Each system has benefits and disadvantages when attempting to make continuous observations of CO_2 flux through snow in cold and remote environments. The flux gradient system can be created cost-effectively and has similar power requirements to a closed-path eddy covariance system, but our results argue that without additional parameterization for advective transport through snow, such systems are likely to underestimate CO_2 efflux during low-snow and springtime periods when efflux may be large. Eddy covariance systems are costly and observations require extensive post-processing but also provide a means to continuously monitor CO_2 efflux from soil through snow to atmosphere throughout the snow-covered season. It is important to note that eddies at frequencies greater than 10 Hz could not be resolved using our eddy covariance setup and that CO_2 that was transported in higher-frequency eddies could not be measured. Hence, eddy covariance observations likely underestimate CO_2 flux to the atmosphere. It is also important to note that all approaches measure CO_2 efflux at effectively a point or a small footprint (on the order of meters), whereas the spatial dynamics of efflux in heterogeneous environments is important to quantify carbon budgets of larger areas. In this case, multiple flux gradient systems can be installed for a similar cost to a single eddy covariance system, but the potential for flux underestimation must be acknowledged. Future studies should seek simple parameterizations for the advective flows through snow that are applicable across ecosystems and be cognizant of the finding that the frequency at which variations in wind velocity induce changes to subnivean $[CO_2]$ occur on time scales of ten hours or longer.

Acknowledgements

We acknowledge logistical support, advice, and fieldwork assistance from Ed Adams, Dan Miller, John Dore, Kelsey Jencso, Ryan Emmanuel, Fabian Nippgen, Vince Pacific, Diego Riveros-Iregui, Padraic Stoy, and Aiden Johnson. The Montana Institute on Ecosystems provided financial assistance. PCS acknowledges funding from the National Science Foundation ('Scaling ecosystem function: Novel Approaches from MaxEnt and Multiresolution', Division of Biological Infrastructure no. 1021095), the Montana Institute on Ecosystems, and the State of Montana. This work was supported by the USDA National Institute of Food and Agriculture Hatch project 228396. Amy Trowbridge provided valuable comments on the manuscript, and we are indebted to Matteo Detto and Victor Venema for providing code for the spectral Granger causality and IAAFT analyses, respectively.

References

Baldocchi, D.D., 2008. "Breathing" of the terrestrial biosphere: lessons learned from a global network of carbon dioxide flux measurements systems, Turner Review. Aust. J. Bot. 56, 1–26.

Barford, C.C., Wofsy, S.C., Goulden, M.L., et al., 2001. Factors controlling long- and short-term sequestration of atmospheric CO_2 in a mid-latitude forest. Science 294 (80-), 1688–1691.

Björkman, M.P., Morgner, E., Cooper, E.J., et al., 2010. Winter carbon dioxide effluxes from Arctic ecosystems: an overview and comparison of methodologies. Glob. Biogeochem. Cycles 24, 1–10. http://dx.doi.org/10.1029/2009GB003667.

Bowling, D.R., Massman, W.J., 2011. Persistent wind-induced enhancement of diffusive CO_2 transport in a mountain forest snowpack. J. Geophys. Res. 116, 1–15. http://dx.doi.org/10.1029/2011JG001722.

Clarke, G.K.C., Waddington, E.D., 1991. A three-dimensional theory of wind pumping. J. Glaciol. 37, 89–96.

Coyne, P.I., Kelley, J.J., 1971. Release of carbon dioxide from frozen soil to the arctic atmosphere. Nature 234, 407–408. http://dx.doi.org/10.1038/234407a0.

Daly, E., Palmroth, S., Stoy, P.C., et al., 2009. The effects of elevated atmospheric CO_2 and nitrogen amendments on subsurface CO_2 production and concentration dynamics in a maturing pine forest. Biogeochemistry 94, 271–287.

Detto, M., Molini, A., Katul, G., et al., 2012. Causality and persistence in ecological systems: a nonparametric spectral Granger causality approach. Am. Nat. 179, 524–535.

Eisenberg, D.S., Kauzmann, W., 1969. The structure and properties of water. Clarendon Press Oxford, Oxford, UK 296 pp.

Eisenberg, D.S., Kauzmann, W., 2005. The structure and properties of water. Clarendon Press, London.

Farnes, P.E., 1995. Comparisons of hydrology, geology, and physical characteristics between Tenderfoot Creek Experimental Forest (east side) Montana, and Coram Experimental Forest (west side) Montana. Montana State University, College of Letters and Sciences, Department of Earth Sciences.

Geweke, J., 1982. Measurement of linear dependence and feedback between multiple time series. J. Am. Stat. Assoc. 77, 304–313.

Goulden, M.L., Daube, B.C., Fan, S.-M., et al., 1997. Physiological responses of a black spruce forest to weather. J. Geophys. Res. 102, 28987–28996.

Granger, C.W.J., 1969. Investigating causal relations by econometric models and cross-spectral methods. Econometrica 37, 424–438.

Grogan, P., Jonasson, S., 2006. Ecosystem CO_2 production during winter in a Swedish subarctic region: the relative importance of climate and vegetation type. Glob. Chang. Biol. 12, 1479–1495. http://dx.doi.org/10.1111/j.1365-2486.2006.01184.x.

Huwald, H., Selker, J.S., Tyler, S.W., et al., 2012. Carbon monoxide as a tracer of gas transport in snow and other natural porous media. Geophys. Res. Lett. 39, L02504.

Jencso, K.G., McGlynn, B.L., Gooseff, M.N., et al., 2009. Hydrologic connectivity between landscapes and streams: transferring reach- and plot-scale understanding to the catchment scale. Water Resour. Res. 45, 1–16. http://dx.doi.org/10.1029/2008WR007225.

Larsen, K.S., Ibrom, A., Jonasson, S., et al., 2007. Significance of cold-season respiration and photosynthesis in a subarctic heath ecosystem in northern Sweden. Glob. Chang. Biol. 13, 1498–1508.

Lee, X., Finnigan, J., Paw, U.K.T., 2005. Coordinate systems and flux bias error. Handb Micrometeorologypp. 33–66.

Liptzin, D., Williams, M.W., Helmig, D., et al., 2009. Process-level controls on CO_2 fluxes from a seasonally snow-covered subalpine meadow soil, Niwot Ridge, Colorado. Biogeochemistry 95, 151–166. http://dx.doi.org/10.1007/s10533-009-9303-2.

Massman, W.J., 1998. A review of the molecular diffusivities of H_2O, CO_2, CH_4, CO, O_3, SO_2, NH_3, N_2O, NO, and NO_2 in air, O_2 and N_2 near STP. Atmos. Environ. 32, 1111–1127.

Massman, W.J., 2006. Advective transport of CO_2 in permeable media induced by atmospheric pressure fluctuations: 1. An analytical model. J. Geophys. Res. 111, G03004.

Massman, W.J., Frank, J.M., 2006. Advective transport of CO_2 in permeable media induced by atmospheric pressure fluctuations: 2. Observational evidence under snowpacks. J. Geophys. Res. 111, G03005.

Massman, W.J., Sommerfeld, R.A., 1997. A model investigation of turbulence-driven pressure-pumping effects on the rate of diffusion of CO_2, N_2O, and CH_4 through layered snowpacks. J. Geophys. Res. 102, 18851–18863. http://dx.doi.org/10.1029/97JD00844.

Mast, M., Wickland, K., 1998. Winter fluxes of CO_2 and CH_4 from subalpine soils in Rocky Mountain National Park, Colorado. Glob. Biogeochem. Cycles 12, 607–620.

Mauder, M., Foken, T., 2004. Documentation and instruction manual of the eddy covariance software package TK2. Univ., Abt. Mikrometeorologie.

McDowell, N.G., Marshall, J.D., Hooker, T.D., Musselman, R., 2000. Estimating CO_2 flux from snowpacks at three sites in the Rocky Mountains. Tree Physiol. 20, 745–753.

Merbold, L., Rogiers, N., Eugster, W., 2012. Winter CO_2 fluxes in a sub-alpine grassland in relation to snow cover, radiation and temperature. Biogeochemistry 111, 287–302.

Merbold, L., Steinlin, C., Hagedorn, F., 2013. Winter greenhouse gas emissions (CO_2, CH_4 and N_2O) from a sub-alpine grassland. Biogeosci. Discuss. 10, 401–445.

Millington, R.J., 1959. Gas diffusion in porous media. Science 130 (80-), 100–120.

Millington, R.J., Quirk, J.P., 1961. Permeability of porous solids. Trans. Faraday Soc. 57, 1200–1207.

Misson, L., Baldocchi, D.D., Black, T.A., et al., 2007. Partitioning forest carbon fluxes with overstory and understory eddy-covariance measurements: A synthesis based on FLUXNET data. Agric. For. Meteorol. 144, 14–31.

Molini, A., Katul, G.G., Porporato, A., 2010. Causality across rainfall time scales revealed by continuous wavelet transforms. J. Geophys. Res. 115, D14123.

Moncrieff, J.B., Massheder, J.M., De Bruin, H., et al., 1997. A system to measure surface fluxes of momentum, sensible heat, water vapour and carbon dioxide. J. Hydrol. 188, 589–611.

Moncrieff, J., Clement, R., Finnigan, J., Meyers, T., 2005. Averaging, detrending, and filtering of eddy covariance time series. In: Lee, X., Massman, W., Law, B.E. (Eds.), Handb. Micrometeorology. Springer, pp. 7–31.

Monson, R.K., Burns, S.P., Williams, M.W., et al., 2006a. The contribution of beneath-snow soil respiration to total ecosystem respiration in a high-elevation, subalpine forest. Glob. Biogeochem. Cycles 20, 1–13. http://dx.doi.org/10.1029/2005GB002684.

Monson, R.K., Lipson, D.L., Burns, S.P., et al., 2006b. Winter forest soil respiration controlled by climate and microbial community composition. Nature 439, 711–714.

Oechel, W.C., Vourlitis, G.L., Brooks, S., et al., 1998. Intercomparison among chamber, tower and aircraft net CO_2 and energy fluxes measured during the Arctic System Science Land-Atmospere-Ice Interactions (ARCSS-LAII) flux study. J. Geophys. Res. 103, 28933–29003.

Pacific, V.J., McGlynn, B.L., Riveros-Iregui, D.A., et al., 2008. Variability in soil respiration across riparian-hillslope transitions. Biogeochemistry 91, 51–70.

Pacific, V.J., McGlynn, B.L., Riveros-Iregui, D.A., et al., 2009. Differential soil respiration responses to changing hydrologic regimes. Water Resour. Res. 45, 6–11. http://dx.doi.org/10.1029/2009WR007721.

Pacific, V.J., McGlynn, B.L., Riveros-Iregui, D.A., et al., 2011. Landscape structure, groundwater dynamics, and soil water content influence soil respiration across riparian-hillslope transitions in the Tenderfoot Creek Experimental Forest, Montana. Hydrol. Process. 25, 811–827. http://dx.doi.org/10.1002/hyp.7870.

Papale, D., Reichstein, M., Aubinet, M., et al., 2006. Towards a standardized processing of Net Ecosystem Exchange measured with eddy covariance technique: algorithms and uncertainty estimation. Biogeosciences 3, 571–583.

Raich, J.W., Potter, C.S., Bhagawati, D., 2002. Interannual variability in global soil respiration, 1980–94. Glob. Chang. Biol. 8, 800–812.

Reichstein, M., Falge, E., Baldocchi, D., et al., 2005. On the separation of net ecosystem exchange into assimilation and ecosystem respiration: review and improved algorithm. Glob. Chang. Biol. 11, 1424–1439.

Riveros-Iregui, D.A., McGlynn, B.L., 2009. Landscape structure control on soil CO_2 efflux variability in complex terrain: scaling from point observations to watershed scale fluxes. J. Geophys. Res. 114, 1–14. http://dx.doi.org/10.1029/2008JG000885.

Riveros-Iregui, D.A., Emanuel, R.E., Muth, D.J., et al., 2007. Diurnal hysteresis between soil CO2 and soil temperature is controlled by soil water content. Geophys. Res. Lett. 34, 1–5. http://dx.doi.org/10.1029/2007GL030938.

Riveros-Iregui, D.A., McGlynn, B.L., Epstein, H.E., Welsch, D.L., 2008. Interpretation and evaluation of combined measurement techniques for soil CO_2 efflux: discrete surface chambers and continuous soil CO_2 concentration probes. J. Geophys. Res. 113, 1–11. http://dx.doi.org/10.1029/2008JG000811.

Riveros-Iregui, D.A., McGlynn, B.L., Marshall, L.A., et al., 2011. A watershed-scale assessment of a process soil CO_2 production and efflux model. Water Resour. Res. 47, 1–12. http://dx.doi.org/10.1029/2010WR009941.

Schäfer, K.V.R., Oren, R., Ellsworth, D.S., et al., 2003. Exposure to an enriched CO_2 atmosphere alters carbon assimilation and allocation in a pine forest ecosystem. Glob. Chang. Biol. 9, 1378–1400.

Schlesinger, W.H., Andrews, J.A., 2000. Soil respiration and the global carbon cycle. Biogeochemistry 48, 7–20.

Schreiber, T., Schmitz, A., 1996. Improved surrogate data for nonlinearity tests. Phys. Rev. Lett. 77, 635–638.

Schreiber, T., Schmitz, A., 2000. Surrogate time series. Phys. D Nonlinear Phenom. 142, 346–382.

Seok, B., Helmig, D., Williams, M.W., et al., 2009. An automated system for continuous measurements of trace gas fluxes through snow: an evaluation of the gas diffusion method at a subalpine forest site, Niwot Ridge, Colorado. Biogeochemistry 95, 95–113.

Serreze, M.C., Clark, M.P., Armstrong, R.L., et al., 1999. Characteristics of the western United States snowpack from snowpack telemetry (SNOTEL) data. Water Resour. Res. 35, 2145–2160.

Sommerfeld, R.A., Mosier, A.R., Musselman, R.C., 1993. CO_2, CH_4 and N_2O flux through a Wyoming snowpack and implications for global budgets. Nature 361, 140–142.

Stoy, P.C., Katul, G.G., Siqueira, M.B.S., et al., 2006. An evaluation of models for partitioning eddy covariance-measured net ecosystem exchange into photosynthesis and respiration. Agric. For. Meteorol. 141, 2–18. http://dx.doi.org/10.1016/j.agrformet.2006.09.001.

Striegl, R.G., Ishii, A.L., 1989. Diffusion and consumption of methane in an unsaturated zone in north-central Illinois, USA. J. Hydrol. 111, 133–143.

Venema, V., Ament, F., Simmer, C., 2006. A stochastic iterative amplitude adjusted Fourier transform algorithm with improved accuracy. Nonlinear Process. Geophys. 13, 321–328.

Vickers, D., Mahrt, L., 1997. Quality control and flux sampling problems for tower and aircraft data. J. Atmos. Ocean. Technol. 14, 512–526.

Wang, T., Ciais, P., Piao, S.L., et al., 2011. Controls on winter ecosystem respiration in temperate and boreal ecosystems. Biogeosciences 361, 2009–2025.